

# MALDI Mass Spectrometry Imaging sample preparation with wet-interface matrix deposition for lipid analysis.

Przemyslaw Mielczarek<sup>1</sup>, Piotr Suder<sup>2</sup>, Paulina Kret<sup>2</sup>, Tymoteusz Słowik<sup>3</sup>, Ewa Ewa Gibuła-Tarłowska<sup>3</sup>, Jolanta Kotlinska<sup>4</sup>, Igor Kotsan<sup>2</sup>, and Anna Bodzoń-Kuśakowska<sup>2</sup>

<sup>1</sup>Maj Institute of Pharmacology Polish Academy of Sciences

<sup>2</sup>AGH University of Science and Technology

<sup>3</sup>Medical University of Lublin

<sup>4</sup>Medical University

March 11, 2023

## Abstract

**RATIONALE:** Sample preparation is one of the most crucial steps for MALDI mass spectrometry imaging (MALDI-MSI). The scientists beginning their adventure with this technique may be overwhelmed by the variety of matrices, solvents, concentrations, the ways of their applications, and the lack of widely available knowledge about the influence of these parameters on the results. Here we would like to present our experiences with detailed aspects of matrices deposition, hopefully helpful for the scientific community. **METHODS:** In our article, we have tested several MALDI matrices applied by the SunCollect® system: wet-interface matrix deposition in the context of lipids analysis. Among them: 2,5-dihydroxybenzoic acid (DHB), norharmane, N-(1-naphthyl) ethylenediamine dihydrochloride (NEDC), 9-aminoacridine (9AA). We have optimized the number of matrix layers and nozzle settings in terms of spectra intensity and the overall quality of obtained ion maps. **RESULTS:** Our research presents the influence of the number of matrix layers and nozzle settings on the results and allows for choosing the optimal parameters for the analyses. In positive ionization mode, DHB matrix could be chosen as the first selection. In the negative ionization mode, DAN matrix produces higher peak intensity in a lower mass range and seems to provide more information than 9AA. We recommended NEDC for particular tasks such as glucose analysis. Comparably to remaining matrices, norharmane significantly changes received ion maps. **CONCLUSIONS:** Dealing with such a great amount of data allows us to notice an interesting conclusion: the obtained ion picture for a particular ion could differ dramatically with changing the matrix, the solvent composition, or even the number of matrix layers. This must be considered when interpreting the result and forces us to compare the results obtained with different matrices with extreme caution.

## Introduction

Sample preparation is one of the most crucial steps in every analytical procedure. Optimization of this part of the experiment is usually the most time-consuming task. Nevertheless, once successfully optimized, the procedure allows for certain and repetitive analyses. Sample preparation for MALDI-MSI is connected to the application of a special matrix before the analysis. The scientists beginning their adventure with this complex and powerful technique may be overwhelmed by the variety of matrices, solvents, concentrations, the ways of their applications, and the lack of widely available knowledge about the influence of these parameters on the final results. Some data can be found in the research articles, technical reports, or protocols provided by the equipment manufacturers, but usually, it is not easy to find a comprehensive recommendation on which matrix and sample preparation strategy to select.

In our study, we decided to use common matrices like 2,5-dihydroxybenzoic acid (DHB), 9-aminoacridine (9AA), 1,5-diaminonaphthalene (DAN), and not as well-known matrices as norharmane and N-(1-naphthyl)

ethylenediamine dihydrochloride (NEDC) to compare their ability to visualize lipids and in some cases (NEDC matrix) small molecules.

To apply matrices, we used SunCollect® system, which utilizes a high-performance pneumatic sprayer. It is recognized as a wet-interface system, and it is worth to mention that its performance may be different from the systems based for example on sublimation process<sup>1</sup> (see: supplementary materials from mentioned article). In this device, the matrix solution could be sprayed in several layers over the tissue sample and from different heights over the sample. The higher position (e.g., topmost position Z=1) produces the driest vapor resulting in the finest matrix crystals size. At the lowest position (Z = 25 mm), the wetter, atomized spray will attain the target. It means that the matrix solution could penetrate the tissue sample and allows to observe the substances that must be extracted from the tissue. In our study, four different positions of the spraying nozzle above the sample surface and the influence of the multiple matrix layers on the quality of obtained MS spectra were examined for each matrix.

DHB matrix is the most common one for the analysis in the positive ionization mode. In the literature different matrix concentration (from 7 mg/ml<sup>2</sup>, to even 50 mg/ml<sup>3</sup> could be applied. Different solvents are used as well. Mainly methanol (MeOH)<sup>4</sup> and acetonitrile (ACN)<sup>5,6</sup> but also ethanol<sup>7</sup> and mixtures of chloroform and methanol<sup>8</sup> are used. 9AA is a popular matrix for the negative ionization mode. In this case, concentration between 2 mg/ml<sup>9</sup> and 10 mg/ml<sup>10</sup> are used, but the most commonly selected is 7 mg/ml (like in<sup>11-13</sup>). Regarding the solvents, mainly aqueous solutions of methanol and ethanol are used in different concentrations. Norharmane and NEDC are still gaining their popularity so, there is no such diversity in their use. In both cases, 7mg/ml is the most popular concentration<sup>13</sup>. Regarding norharmane for SunCollect® application, the concentration of 6 mg/ml and the solution of chloroform: MeOH:H<sub>2</sub>O, 1:2:0.8 (v/v/v) is used since in given volumes ratios, the solution creates a homogenous mixture, and separation of water and chloroform is not observed. Additionally, 1.5-DAN (25 mg/ml, in ACN:H<sub>2</sub>O, 1:1, v/v)<sup>14</sup> and 1.5 DAN hydrochloride proposed by Liu et al.<sup>15</sup> were tested.

The cross-section of a rat spinal cord was chosen as a tissue model, representing the features of the central nervous system. Particularly, its simple structural division into a gray and white matter should be easily recognizable on MSI tissue scans. Additionally, the slices obtained from this tissue are small and thus convenient for the fast MSI measurements. Thickness of the slides was typical for most MALDI-MSI experiments and was set to 12 µm. To compare different matrices, we decided to choose several different peaks representing lipids from the spinal cord's gray and white matter, well known in the literature<sup>16-18</sup>. Such choice allows for visualization of the structures and comparing the quality of obtained results between different matrices. Additionally, the care was taken to choose intensive, as well as relatively small, peaks to show their behavior in the broad intensity range (see Fig.1). Finally, the parameters of chosen peaks, especially their intensities, were used for the comparison.

## Hosted file

image1.emf available at <https://authorea.com/users/594870/articles/629130-maldi-mass-spectrometry-imaging-sample-preparation-with-wet-interface-matrix-deposition-for-lipid-analysis>

**Fig. 1** Examples of averaged mass spectra from the rat spinal cord slices measured in positive (A) and negative (B) ionization modes. The peaks used in the analysis and comparison of different matrices have been signed in the figure.

## Materials and Methods

### Tissue preparation

All experiments on animals were performed according to the respective Polish and European Communities Council Directives (86/609/EEC) and were approved by the local Ethics Committee (approval number 137/2018). The tissues were obtained as spared from control animals used during other experiments, according to the so-called 3R (replacement/reduction/ refinement) rule. Immediately after isolation, the rat

spinal cords were flash frozen and kept in a liquid nitrogen storage dewar (LS750, Worthington Industries, Columbus, OH, USA) until assayed. Approximately 1 h before cutting, the tissue was transferred to the cryomicrotome chamber (Cryotome FSE, Thermo Fisher Scientific, Chesire, UK). Both, the chamber, and the specimen temperatures were set to  $-15^{\circ}\text{C}$ . Slices were cut at  $12\ \mu\text{m}$  slices, and immediately thaw-mounted on the indium-tin oxide (ITO) glasses (Bruker-Daltonics, Bremen, Germany). The tissue slices were then vacuum-dried for about 45 min. Prepared samples were stored in a laboratory freezer at  $-80^{\circ}\text{C}$  (NU9483, NuAire Inc., Plymouth, MN, USA) in the hermetically sealed boxes. Just before analysis, the samples were warmed up to an ambient temperature in a vacuum desiccator to prevent moisture condensation on the sample's surface and dried again for about 45 min. Before each matrix deposition, an optical image (600 dpi) of the tissue cross-sections with marked fiducials was recorded.

Additionally, as suggested by Angel et al.<sup>19</sup>, before analysis in both modes (pos./neg.), tissue washing by 50 mM ammonium acetate  $\text{pH} = 6.5$  by 10 s has been tested. This procedure is suggested, especially in the negative ionization mode, as a way to improve the sensitivity of the measurements.

### **MALDI matrices:**

During the experiments, the following chemicals were used: solvents: ACN and MeOH (J.T. Baker, Amsterdam, Netherlands), both at the HPLC gradient grade, ethanol (Avantor, Poland) chloroform, ultrapure water (Sigma-Aldrich/Merck, Germany). Matrices: 2,5-dihydroxybenzoic acid (DHB), trifluoroacetic acid (TFA), norharmane, N-(1-naphthyl) ethylenediamine dihydrochloride (NEDC) all from Sigma-Aldrich/Merck (Darmstadt, Germany).

### **Matrix application:**

The matrices were applied by a SunCollect(r) device (SunChrom GmbH, Friedrichsdorf, Germany). The flow rate of the matrix solution changed among layers, according to the manufacturer recommendations: 10  $\mu\text{L}/\text{min}$  for the first layer, 20  $\mu\text{L}/\text{min}$  for the second layer, 30  $\mu\text{L}/\text{min}$  for the third layer, 40  $\mu\text{L}/\text{min}$  for the fourth layer, and 60  $\mu\text{L}/\text{min}$  for all following layers. The nozzle applied the matrix solution with a line distance of 2 mm, and the speed 600 mm/min. For each matrix, a different number of layers was applied. The Z value – the position of the spraying nozzle above the tissue surface was also tested.  $Z=1$  means the highest possible (about 50 mm) position above the tissue, whereas  $Z=25$  means about 25mm above the tissue and is determined as the “extraction mode”. Four different numbers of layers and four different nozzle heights were tested for each matrix.

### **MALDI measurements**

Matrix-coated sections were subjected to imaging experiments using the MALDI-TOF/TOF UltrafleXtreme MS (Bruker-Daltonics, Bremen, Germany) with a Smartbeam II laser operating at 2 kHz. All following MS parameters underwent initial, multistep optimization. Ions were accelerated at 25 kV with a pulsed ion extraction of 120 ns and ion suppression up to 100 Da. Spectra were recorded in positive and negative ion modes with reflectron, within an 200–3000  $m/z$  range. They were externally calibrated with Peptide Calibration Standard II (Bruker-Daltonics, Bremen, Germany) and known matrix ions, e.g. 273.0399  $m/z$  for DHB matrix ( $[2\text{DHB}-2\text{H}_2\text{O}+\text{H}]^+$  ion) and 229.0533  $m/z$  for 9AA matrix ( $[9\text{AA}+\text{Cl}]^-$  ion). A raster width of 200  $\mu\text{m}$  was applied to all samples. In total, 400 shots were collected from each ablation point with 20 shots at the raster spot, and the laser focus diameter was set to “3\_medium”. FlexControl version 3.4 (Bruker-Daltonics, Bremen, Germany) was employed for spectra acquisition, and FlexImaging, version 4.0 was used for data processing and the creation of molecular images. Mmass software (version 5.5.0, Open-Source software developed by Martin Strohalm, Academy of Sciences, Prague, Czech Republic) was used for the spectra analysis<sup>20</sup>.

### **Results**

To keep this chapter as clear as possible, we divided it into three subchapters: tissue washing (1), matrix spraying nozzle height over the sample, and the number of matrix layers in positive (2) and negative (3) ionization modes. DHB, norharmane, and DAN matrices were tested in the positive ionization mode. In

the negative ionization mode, norharmane, NEDC, and 9AA matrices were used. Below there is a brief description of the optimization procedures.

### Tissue washing

Some Authors recommend applying the tissue washing procedure before analysis to remove substances interfering with the ionization process<sup>19,21</sup>. The procedure is easy: the sample on the ITO glass should be immersed into a solvent a few times and dried. To test this approach, we used the procedure described by Angel et al.<sup>19</sup>: two slices were washed with 50 mM ammonium acetate by immersing them for 10 s and subsequent drying in the desiccator for the next 15 minutes.

After washing, we observed four types of effects influencing the final results:

- (1) some substances were completely washed away: their ions, typically present in non-washed tissue, were not observed,
- (2) the final picture was significantly blurred (see Fig. 2: the difference between both gray and white matters has vanished),
- (3) all peak intensities were elevated (probably due to the removal of substances responsible for the ion suppression effect). However, spectra enhancement did not significantly influence the interpretation of the results.
- (4) The picture for specific  $m/z$  values remains the same before and after washing.

Summing up, washing procedures, if not thoroughly tested to visualize the peaks of interest, usually could not lead to the desired results. It is also important to keep in mind the possibility of delocalization of the molecules and increase the sample variability generated by the washing procedure. So, we decided to perform the measurements in the conditions as unchanged as possible.



**Fig. 2** Blurring effect after tissue washing - the difference between white and gray matter has vanished. Washing: 50 mM ammonium acetate for 10 s, matrix: 25 mg/ml DHB (MeOH:H<sub>2</sub>O 1:1, 0,2% TFA),  $m/z$  718.

The number of matrix layers and the height of the spraying nozzle during matrix application – positive ionization mode (DHB, norharmane, and DAN matrices)

To compare the influence of the different matrix layers and the position of the spraying nozzle on the spectra quality, we decided to select two parameters: the peak intensity (int.) and the signal-to-noise ratio (s/n). Peak intensity alone could be misleading since the increase of the overall spectra intensity may occur simultaneously with the background signal increase, which could, in turn, decrease the s/n value and, in effect, worsen the analysis quality.

### 25 mg/ml DHB matrix (MeOH:H<sub>2</sub>O 1:1, 0,2% TFA) – positive ionization mode

25 mg/ml DHB matrix (50% MeOH, 0.2% TFA) could be treated as a reference matrix in the positive ionization mode. To check the influence of the parameters of matrix application by the SunCollect® system, we have chosen four different numbers of matrix layers (L= 8, 10, 12, 14) and four different heights of the spraying nozzle (Z=25, 15, 5, 1,).

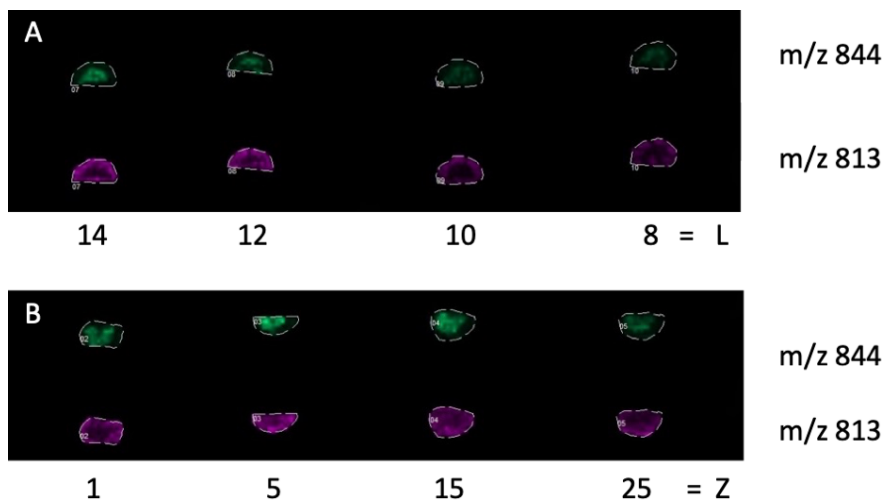


**Fig. 3** The ion map for m/z 844 and m/z 813 obtained from the slices of the spinal cord for DHB matrix with the different number of matrix layers (A) and four different heights of spraying nozzle (B) for the positive ionization mode (matrix: 25 mg/ml DHB (50% MeOH, 0.2% TFA))

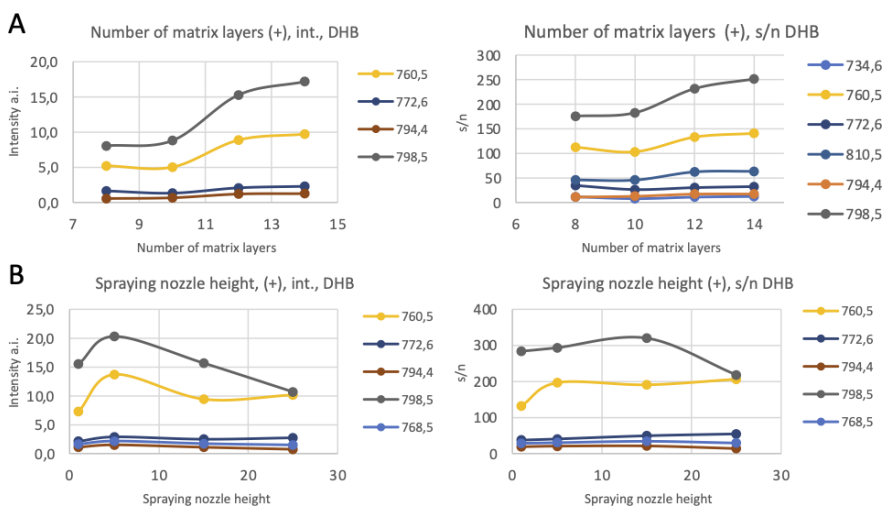


**Fig. 4** The relationship between the chosen peaks' intensities and signal-to-noise ratio (s/n) in terms of the number of matrix layers (A) and the spraying nozzle height (B) for the positive ionization mode, rat spinal cord tissue slices (matrix: 25 mg/ml DHB (50% MeOH, 0.2% TFA))

Considering the ions intensities, the highest increase in those parameters was observed between 10 and 12 layers (see: Fig. 3,4). The parameters for the 12 and 14 layers were similar and did not lead to the further spectra enhancement. The same trend is observed with the s/n value. Thus, we decided that 12 layers would be optimal for the measurements since it allows to save the chemical reagents and time for tissue preparation. The spraying nozzle height of 5 mm gives the highest intensity for observed peaks. For s/n ratio the 5 mm

and 10 mm positions give the maximum value, but the intensity itself is higher for 5 mm. Thus, considering both parameters, the 5 mm position was recommended for the DHB matrix in the positive ionization mode.

### Norharmane (6 mg/ml matrix (chloroform: MeOH:H<sub>2</sub>O) – positive ionization mode)

Norharmane works differently than DHB matrix. For s/n ratio, 12 and 14 layers show high value, but 14 matrix layers are optimal considering the peaks intensities only (see: Fig. 5,6). Regarding the position of the spraying nozzle above the measured sample, the most intensive peaks are obtained both at the highest (z=1) and the lowest position of the spraying nozzle (Z=25), preferably with the lowest position. The same is valid for the s/n ratio.

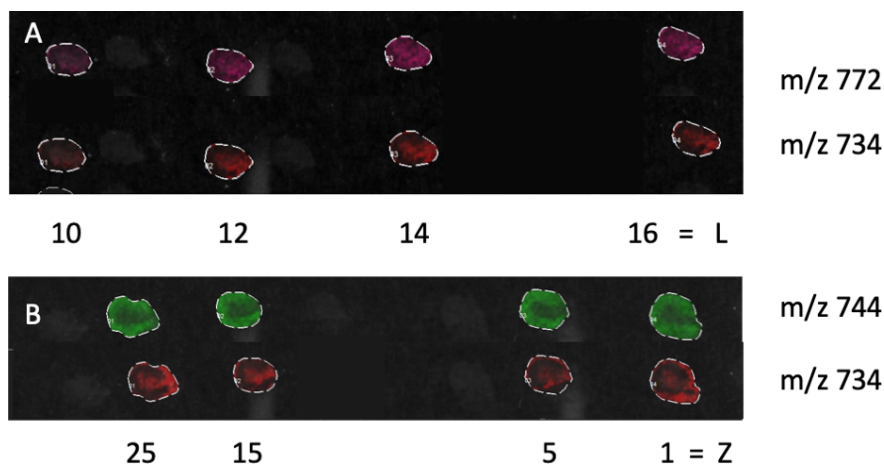


**Fig. 5** The ion map for m/z 772, m/z 734 and m/z 744 obtained from the slices of the spinal cord for norharmane matrix with the different number of matrix layers (A) and four different heights of spraying nozzle (B) for the positive ionization mode (matrix: 6 mg/ml norharmane (chloroform:MeOH:H<sub>2</sub>O))

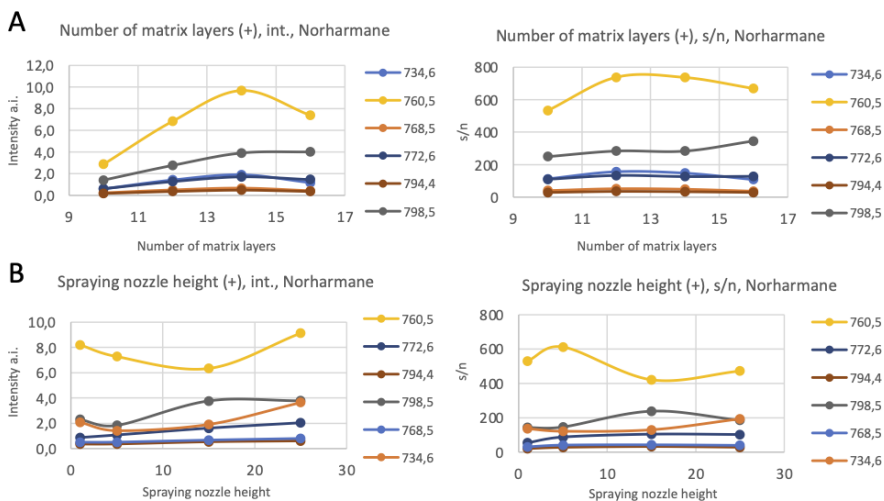


**Fig. 6** The relationship between the chosen peaks' intensities and signal-to-noise ratio (s/n) in terms of the number of matrix layers (A) and the spraying nozzle height (B) for the positive ionization mode rat spinal cord tissue slices (matrix: 6 mg/ml norharmane (chloroform:MeOH:H<sub>2</sub>O))

The problem with that matrix lies in the fact that, for several  $m/z$  values, we obtained different ion maps in comparison with DHB matrix (see discussion chapter).

### DAN (2.5 mg/ml 50% ACN – positive ionization mode)

For this matrix, the highest position of the nozzle ( $z=1$ ) and 16 layers seem to be the best setting when the peaks intensities and the  $s/n$  ratios are considered (see: Fig. 8). But looking at different ion maps (see: Fig. 7), 14 matrix layers seem to give better results. For several ion maps, additional matrix layers blurred the picture. The same is observed for  $z=1$  and  $z=5$ ; thus,  $z=5$  seems the best.

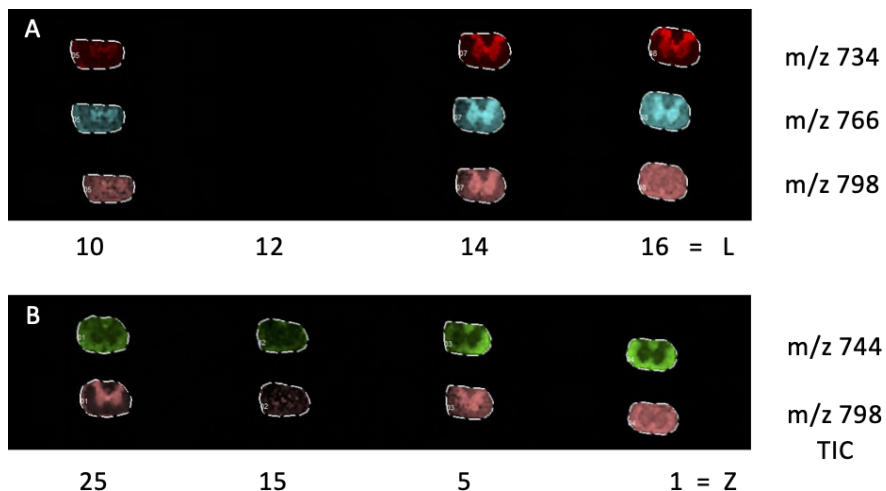


**Fig. 7** The ion map for  $m/z$  734,  $m/z$  766,  $m/z$  798, and  $m/z$  744 obtained from the slices of the spinal cord for the DAN matrix with the different number of matrix layers (A) and four different heights of spraying nozzle (B) for the positive ionization mode (matrix: 2.5 mg/ml DAN 50% ACN). Consider different ion maps for different spraying nozzle heights (Z) and the number of layers (L) in the case of  $m/z$  798.

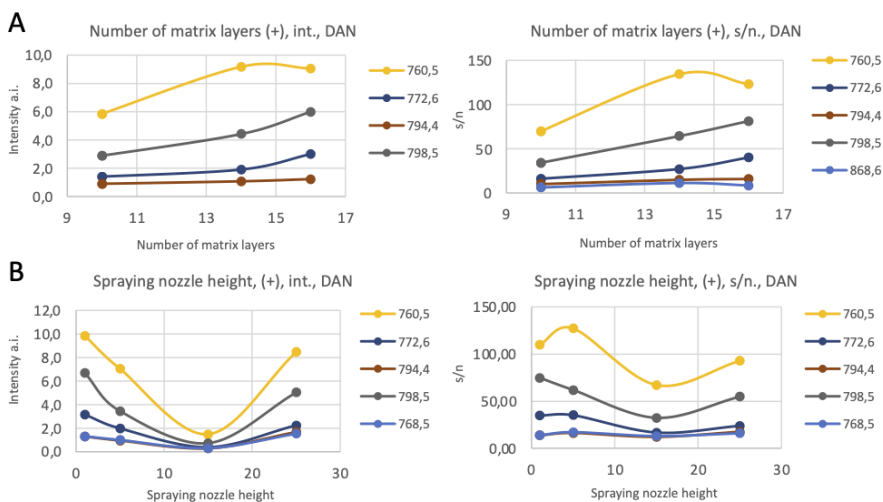


**Fig. 8** The relationship between the chosen peaks' intensities and signal-to-noise ratio ( $s/n$ ) in terms of the number of matrix layers (A) and the spraying nozzle height (B) for the positive ionization mode rat spinal cord tissue slices (matrix: 2.5 mg/ml DAN 50% ACN)

Here we also observe discrepancies between ion maps produced by different matrices (see: discussion).

**The number of layers and the spraying nozzle height – negative ionization mode (9AA, norharmane, NEDC and DAN matrices)**

**9-Aminoacridine (9AA 7 mg/ml 70% EtOH) – negative ionization mode**

Four different numbers of matrix layers ( $l= 10, 12, 14, 16$ ) and four different positions of spraying nozzle height ( $Z=25, 15, 5, 1$ ) were tested for 9AA as a reference matrix in the negative ionization mode. As previously, the peaks intensities and the  $s/n$  ratios were compared.

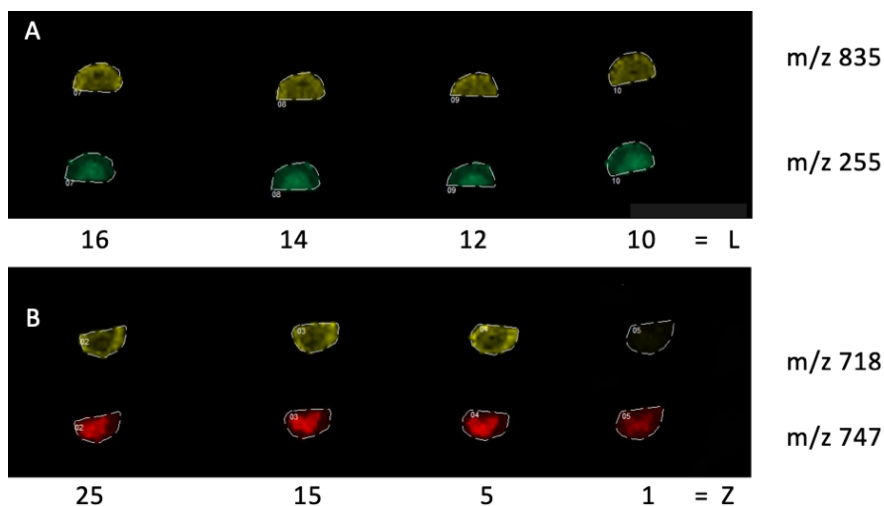


**Fig. 9** The ion map for  $m/z$  835,  $m/z$  255,  $m/z$  718, and  $m/z$  747 obtained from the slices of the spinal cord for 9AA matrix with the different number of matrix layers (A) and four different heights of the spraying nozzle (B) for the negative ionization mode (9AA 7 mg/ml 70% EtOH)

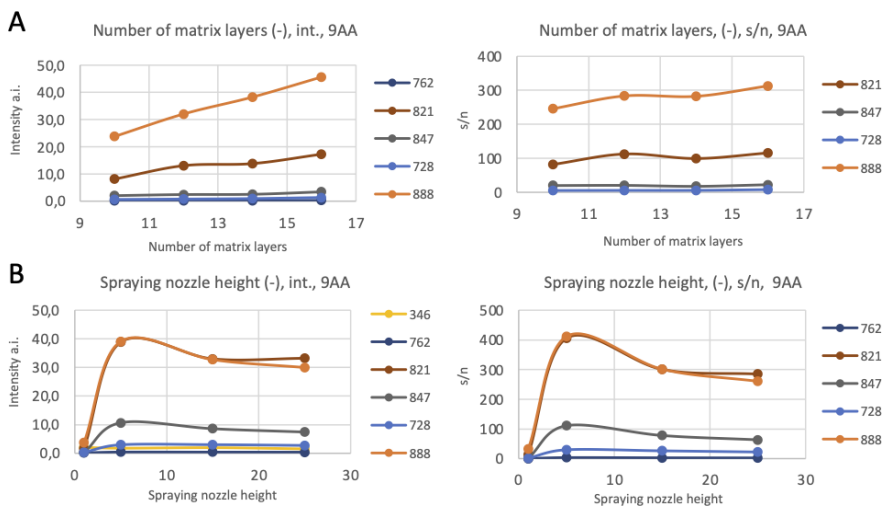


**Fig. 10** The relationship between the chosen peaks' intensities and signal-to-noise ratio ( $s/n$ ) in terms of the number of matrix layers (A) and the spraying nozzle height (B) for the negative ionization mode rat spinal cord tissue slices (matrix: 9AA 7 mg/ml 70% EtOH)

Nozzle height does not significantly affect the quality of the analysis, but the peaks on the spectra are more intensive with the higher position of the nozzle. S/n ratio is definitely higher for a higher nozzle position. Thus  $z=5$  was chosen as the best one. In the case of matrix layers, we observe the increase in the peak's intensity with increasing number of layers (see: Fig. 10). Nevertheless, assessing the quality of the picture, 14 layers seems to be a good choice. With the 16 layers, the picture becomes a little bit blurred (see: Fig. 9). Thus, it is not recommended when we are interested in looking for different brain structures. Additionally, in the case of **14 layers**, stable picture is obtained with different normalization methods, which proves the good quality of the measurement (see: Fig. 11).

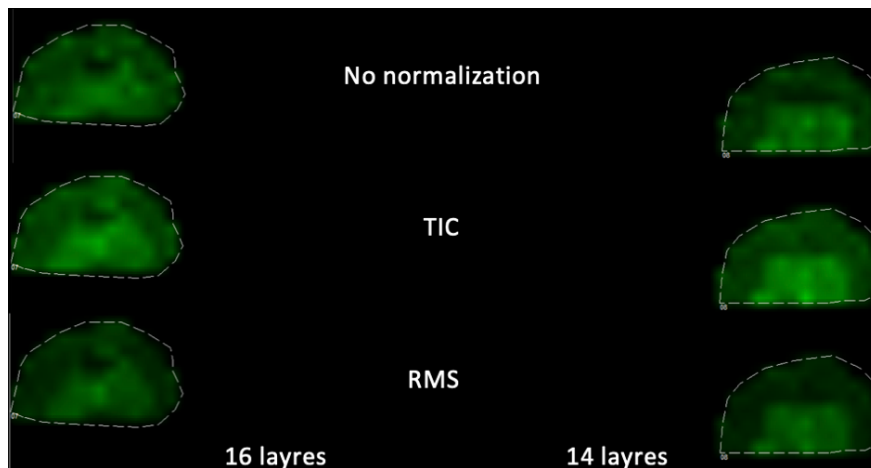


**Fig. 11** The reduced quality of the ion map with increasing number of matrix layers without and with normalization (TIC – total ion current and RMS - root mean squared) – negative ionization mode (9AA 7 mg/ml 70% EtOH).

#### **Norharmane (6 mg/ml matrix (chloroform:MeOH:H<sub>2</sub>O)) – negative ionization mode**

In the case of norharmane (6 mg/ml in chloroform:MeOH:H<sub>2</sub>O, 1:1:1, v/v/v solution) the intensity of the peaks on the spectrum increased with the number of the matrix layers but starting from the 12 layers, further increase was minor. Conversely, the s/n ratio decreases starting from the twelfth layer. Thus, up to 12 matrix layers seem to be optimal. For the spraying nozzle position, 15 mm is performing the best since the intensity, and s/n ratio is relatively high. Lower nozzle position does not change the intensity but might be responsible for the molecule's delocalization (see: Fig 12, 13).

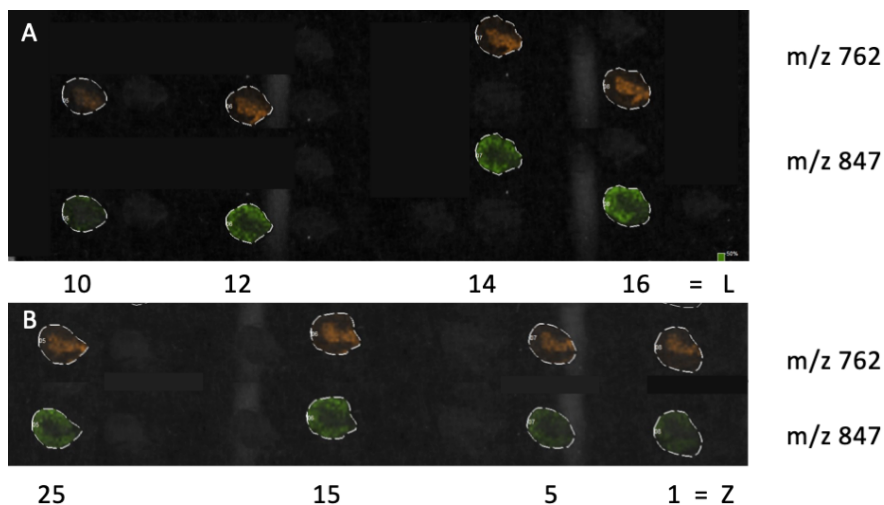


**Fig. 12** The ion map for  $m/z$  762 and  $m/z$  847 obtained from the slices of the spinal cord for norharmane matrix with the different number of matrix layers (A) and four different heights of spraying nozzle (B) for the negative ionization mode (matrix: 6 mg/ml norharmane (chloroform:MeOH:H<sub>2</sub>O))

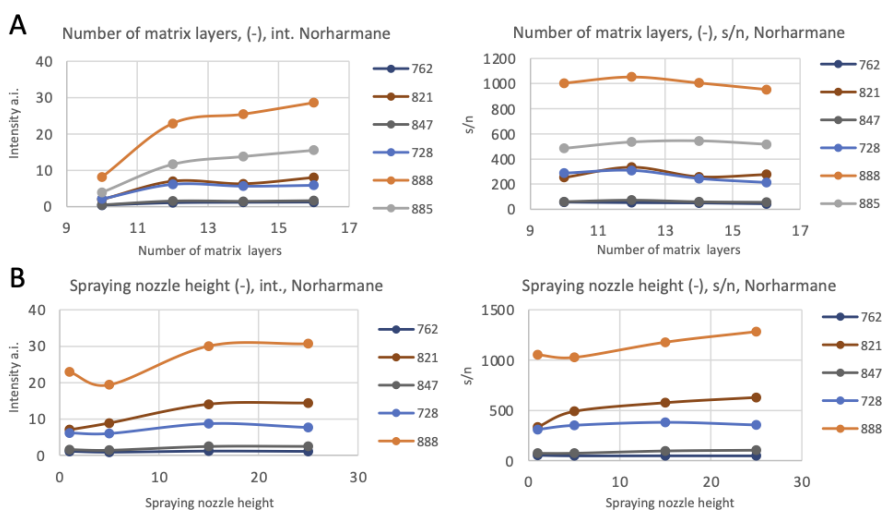


**Fig. 13** The relationship between the chosen peaks' intensities and signal-to-noise ratio ( $s/n$ ) in terms of the number of matrix layers (A) and the spraying nozzle height (B) for the negative ionization mode rat spinal cord tissue slices (matrix: 6 mg/ml norharmane (chloroform:MeOH:H<sub>2</sub>O))

Generally, for the negative ionization mode, norharmane gives the spectra of higher intensity for the lipids around  $m/z = 728$  compared to 9AA and then with the higher  $m/z$  range their intensities are going lower (see: Fig. 21). Additionally, there is no signal observed for low  $m/z$  ions like  $m/z = 255$ , or  $m/z = 283$ . It seems, that only the lipids of higher molecular weights are able to ionize with this matrix.

### N-(1-naphthyl) ethylenediamine dihydrochloride (NEDC) – negative ionization mode

NEDC (7 mg/ml, 70% MeOH) is quite destructive when sprayed from the low position of the spraying nozzle. This effect is seen in Fig. 14. Spraying nozzle heights 25 and 15 gave quite intensive spectra, but the problem with matrix crystallization could be clearly observed in the picture. Therefore, spraying nozzle height at a

value **5** seems to be optimal. It gives quite good peak intensity for small molecules and lipids and the s/n ratio is also acceptable (Fig. 15).

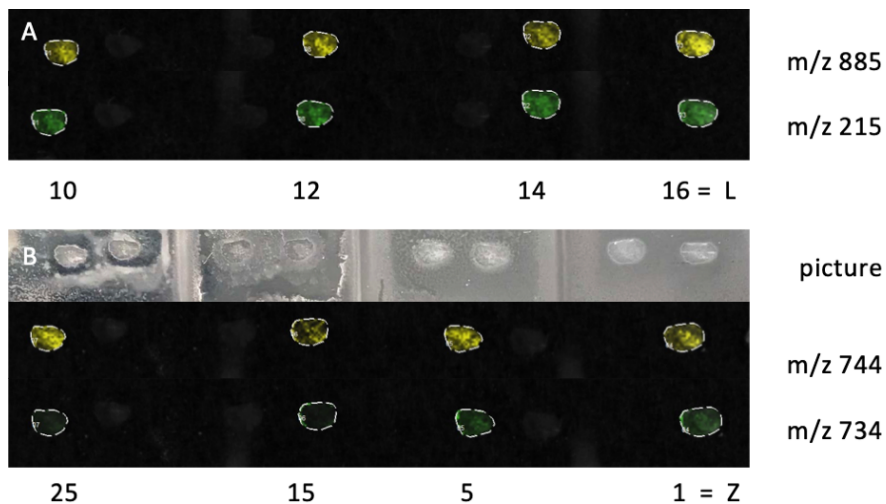


**Fig. 14** The ion map for m/z 885, m/z 215 and m/z 744 and m/z 734 obtained from the slices of the spinal cord for NEDC matrix with the different number of layers (A) and four different heights of spraying nozzle (B) for the negative ionization mode (matrix: 7 mg/ml NEDC, 70% MeOH), (m/z 215 – [glucose +Cl<sup>-</sup>]). Additionally, a picture of the glass covered with NEDC matrix.

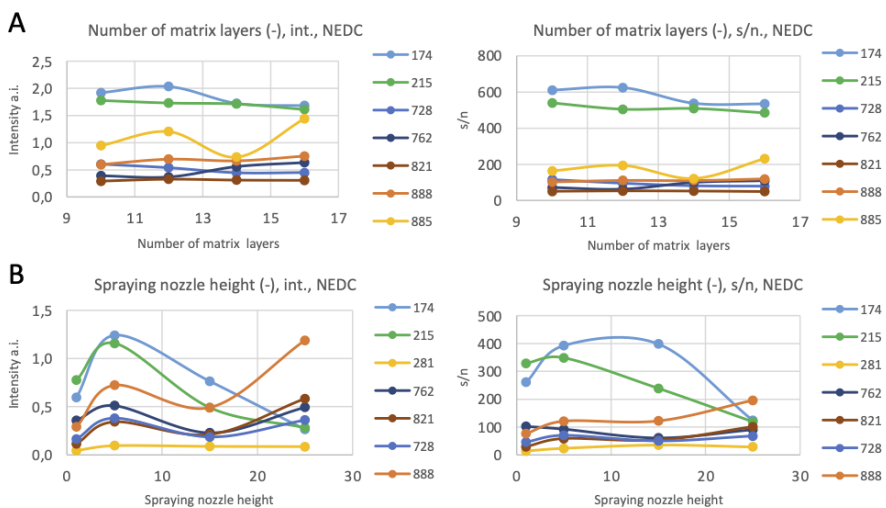


**Fig. 15** The relationship between the chosen peaks' intensities and signal-to-noise ratio (s/n) in terms of the number of matrix layers (A) and the spraying nozzle height (B) for the negative ionization mode rat spinal cord tissue slices (matrix: 7 mg/ml NEDC (70% MeOH) – (m/z 215 – [glucose +Cl<sup>-</sup>]).

NEDC is the only matrix able to decrease peaks intensities with the increasing number of the matrix layers, which is observed for low MW compounds that could be observed with this matrix (see: m/z 215 for glucose and 174 for glucose-3-phosphate (G3P), Fig. 15). Here 10 to 12 matrix layers seem to be optimal. For lipids, the situation depends on a compound. For some of them, the trend is similar, while for others is the opposite. To effectively observe lipids and small molecules, **12** layers seem to be the most promising. It has

to be mentioned that NEDC matrix has the lowest intensity of the three tested matrices in the negative ionization mode with a comparable s/n ratio (Fig. 21).

DAN (2,5 mg/ml 50% ACN – negative ionization mode)

For DAN matrix  $Z = 1$  and  $L = 16$  layers gives the highest intensity, and the trend for s/n ratio is the same. Spraying nozzle height at the highest position gives the best results (Fig. 16,17).

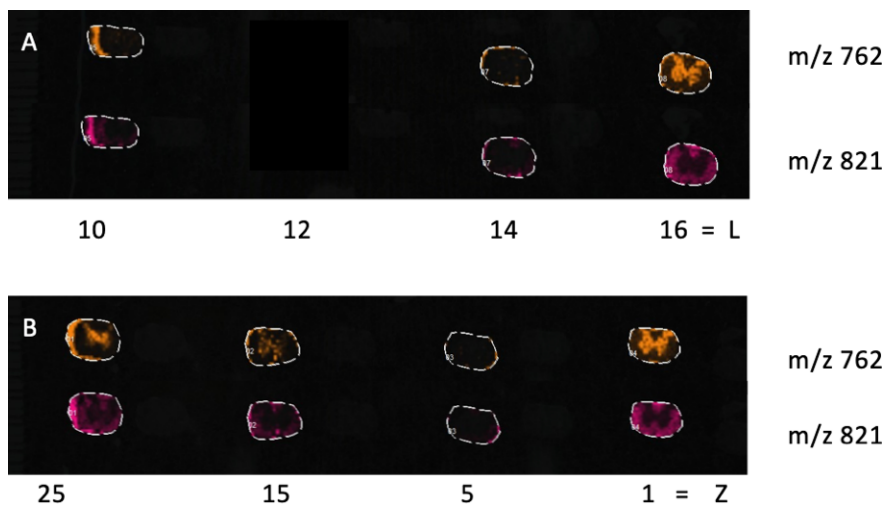


**Fig. 16** The ion map for m/z 762 and m/z 821 obtained from the slices of the spinal cord for DAN matrix with the different number of layers (A) and four different heights of spraying nozzle (B) for the negative ionization mode (matrix: 2.5 mg/ml DAN, 50% ACN)

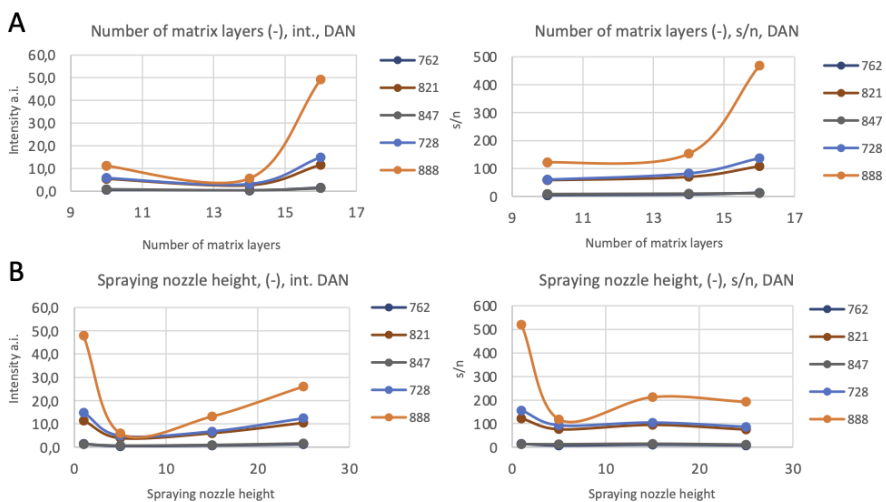


**Fig. 17** The relationship between the chosen peaks' intensities and signal-to-noise ratio (s/n) in terms of the number of matrix layers (A) and the spraying nozzle height (B) for the negative ionization mode rat spinal cord tissue slices (matrix: DAN 2.5 mg/ml 50% ACN).

## Discussion

### 1. Different matrices, different pictures

Collecting such a great amount of analysis allows us to notice an interesting observation: the obtained ion map of a particular ion could differ dramatically regardless of the used matrix, the solvent composition, or even the number of matrix layers.

In the positive ionization mode, we have observed this effect for the norharmane and DAN matrices in comparison with the classical DHB matrix. Norharmane produces a strong signal from lipids. Nevertheless, the lipids seem to be located in a whole tissue area, and the discrimination between the white and the gray matter is lost. For example, the ion map for  $m/z$  810 and 766 for the DHB matrix suggests that those substances are present mainly in the white matter, but in the case of norharmane, these peaks were present all over the tissue slice (see Fig. 18). This effect occurs probably because the chloroform is used as a solvent.

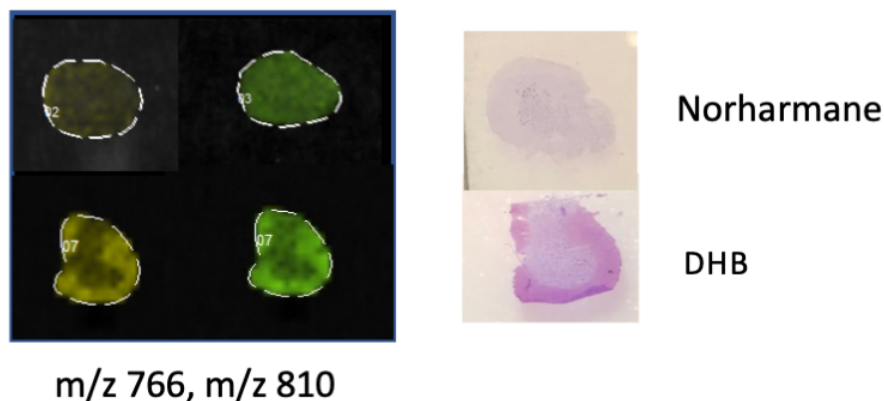


**Fig. 18** The difference in the ion map between norharmane and DHB matrix. The structures visible with the DHB matrix are not present when the norharmane matrix is used. Cresyl violet staining show white and gray matter in the spinal cord slices.

From 11 peaks taken for the analysis, three behaved in that way: in DHB, they can be seen in the white or gray matter, whereas in norharmane their distribution is over the whole tissue ( $m/z = 766, 810,$  and  $872$ ). Surprisingly the ion at  $m/z=798$  in the norharmane matrix shows its distribution in a gray region only. Because of that, the norharmane matrix seems sufficient for the lipids when the differences among the structures are not crucial.

The study of the DAN matrix revealed that the way of sample preparation (the number of matrix layers and the spraying nozzle height) – may also influence the overall picture. In the case of this matrix, three ions:  $m/z$  760, 798, 868 were detected from the gray matter - not from the whole tissue as in the case of the “classical” DHB matrix (see Fig. 19).

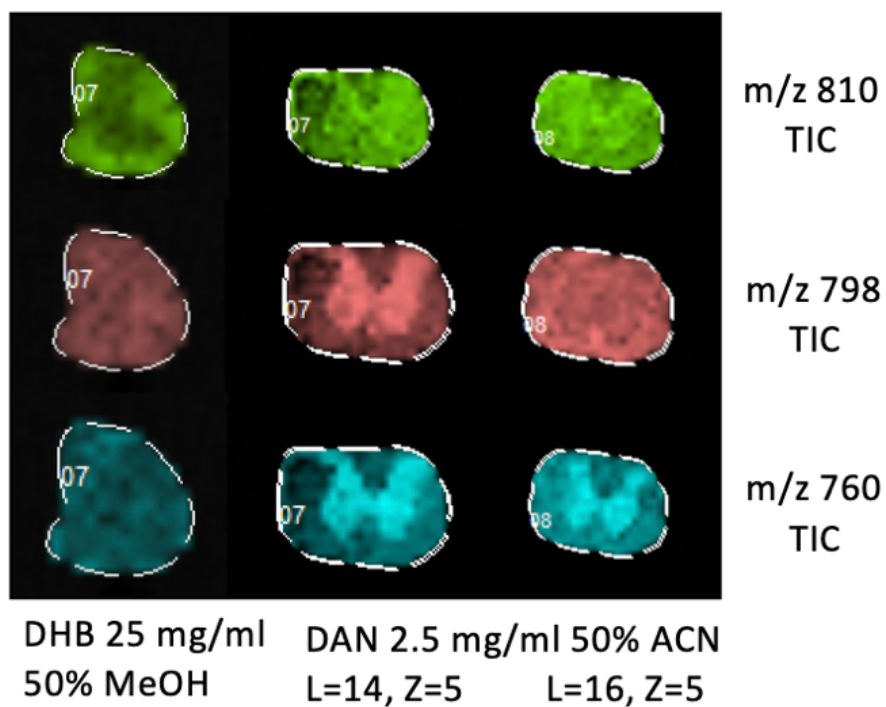


**Fig. 19** Discrepancies between ion maps produced by DHB and DAN matrices in the positive ionization mode.

Similar effects are observed during solvent changes for the same matrix. Exemplary, for the 9AA in 100% methanol, we saw the ion map for m/z 281 on a tissue slice in the white matter only, whereas for the 9AA matrix with 70% ethanol/water solution, the same signal is distributed all over the sample (see: Fig.20).

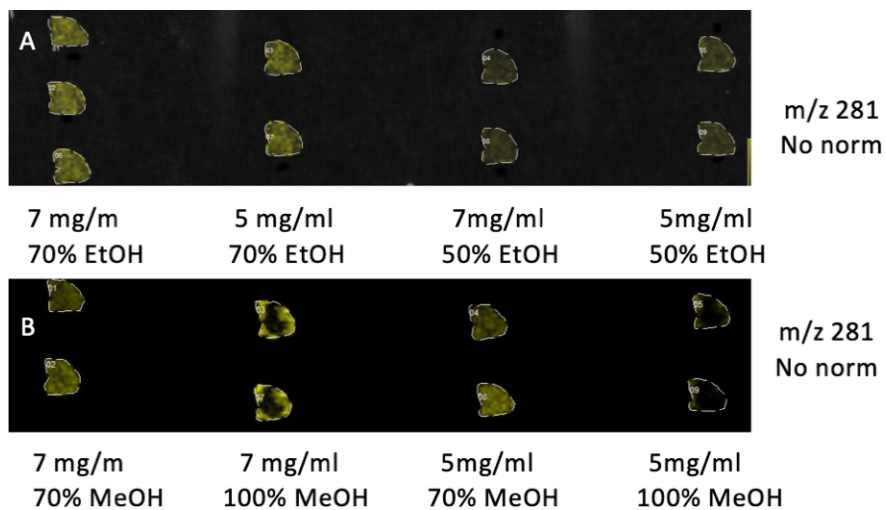


**Fig. 20** The ion map for m/z 281 obtained from the slices of the spinal cord for 9AA matrix with different concentrations of matrix (7 mg/ml 9AA and 5 mg/ml 9AA) and solvent: A - 70% EtOH, 50% EtOH; B - 70% MeOH and 100% MeOH).

Such solvent-related, matrix-related effects must be taken into consideration during the interpretation of the

results. If a single ion seems to be desorbed from a single structure with the aid of exact solvent/matrix mixture, it does not mean that using the other solvent, or matrix will give us the same result. Thus, it should be clearly stated that comparing the ion maps obtained from different matrices and solvents, must be done with extreme caution.

## **2. Technical considerations about wet interface matrix deposition.**

Wet-interface matrix deposition devices allow to control the number of applied matrix layers and the nozzle height over the sample. Our article points the necessity of proper optimization of the process of sample preparation, since it could help to obtain a substantial improvement of the analysis parameters.

### **2.1. The number of applied matrix layers**

In the positive ionization mode for DHB and norharmane matrices, the peaks overall intensity gets higher with the higher number of matrix layers, but only up to some optimum. After that point, the number of layers does not increase the peaks intensity or does it insignificantly. In the case of DAN, the higher number of layers may even be responsible for losing the discrimination between the white and gray matter in the discussed case. Thus, it is highly advisable to check this parameter during sample preparation optimization.

In the negative ionization mode for 9AA and norharmane, the peaks intensity increases with the number of the matrix layers, and we did not observe the “saturation effect.” Nevertheless, the quality of the obtained ion map could be reduced. Thus, this parameter must be optimized before the final analysis. For NEDC matrix and lipid analysis, the effect is very similar, except for small molecules such as glucose. In this case, the lower number of matrix layers gives better results.

### **2.2. The spraying nozzle height above the tissue sample**

The position of the spraying nozzle above the sprayed sample is correlated with the intensity of obtained spectra, but the correlation depends on the matrix type. In the case of DHB, the peaks intensities are higher with the higher position of the nozzle ( $Z=5$ ), but for norharmane, most intensive peaks are obtained at the lowest position ( $Z = 25$ ). The same correlation is for 9AA ( $Z=5$ ) and norharmane ( $Z=15$ ) in the negative ionization mode. Sometimes, the visual effect of matrix application – such as local tissue damage or irregular crystallization – could be observed. Such circumstances determine the proper matrix application, as in the case of the NEDC matrix. Our study clearly shows that such basic optimization is necessary. For example, a higher nozzle height is frequently recommended for the lipid analysis, but unexpectedly for the norharmane lower position works better.

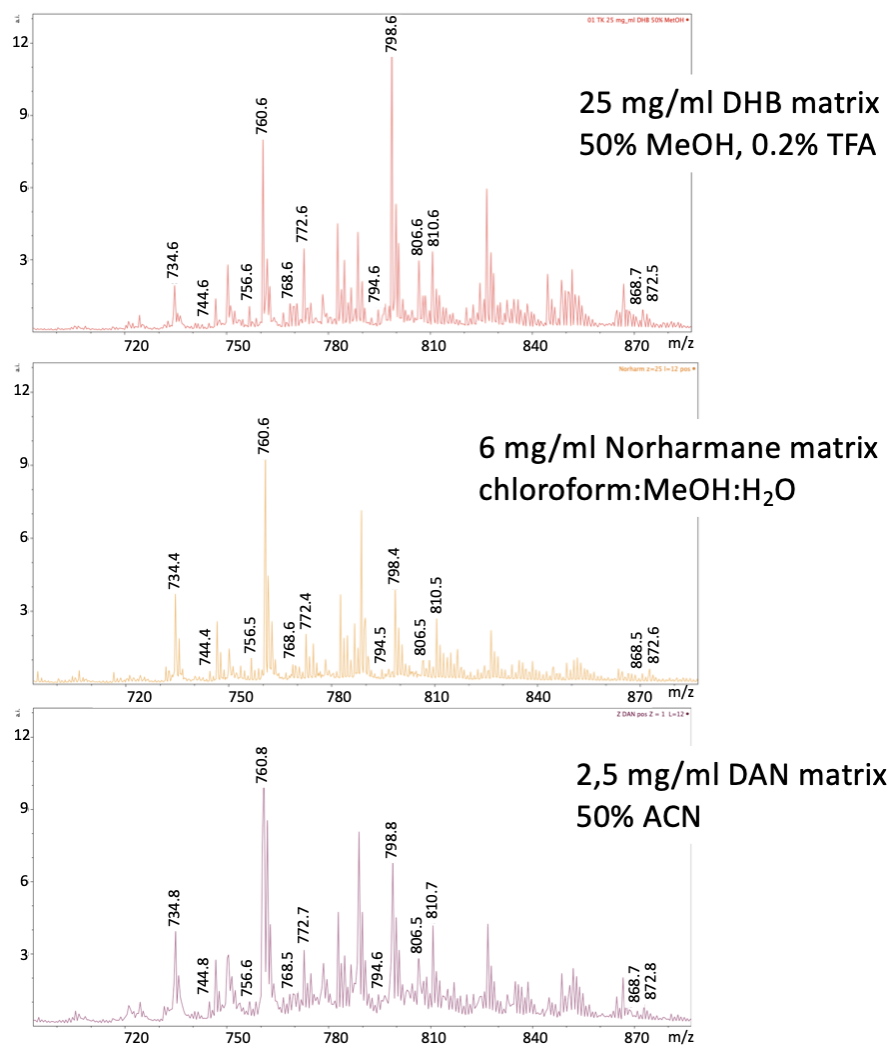


**Fig. 21** The spectra of DHB, DAN and norharmane matrix

Considering quite similar performance of different matrices in positive ionization mode, in our opinion DHB matrix could be chosen as the first selection (see Fig. 21). Norharmane matrix could be rejected since it changes the ion map – probably as a result of the solvent properties. As it was noted, for several m/z values, we obtained different ion maps in comparison with DHB matrix. Generally, DHB matrix gives higher peaks intensity and s/n ratio. Thus, for the measurement of lipids in the positive ion mode, we recommended this matrix.

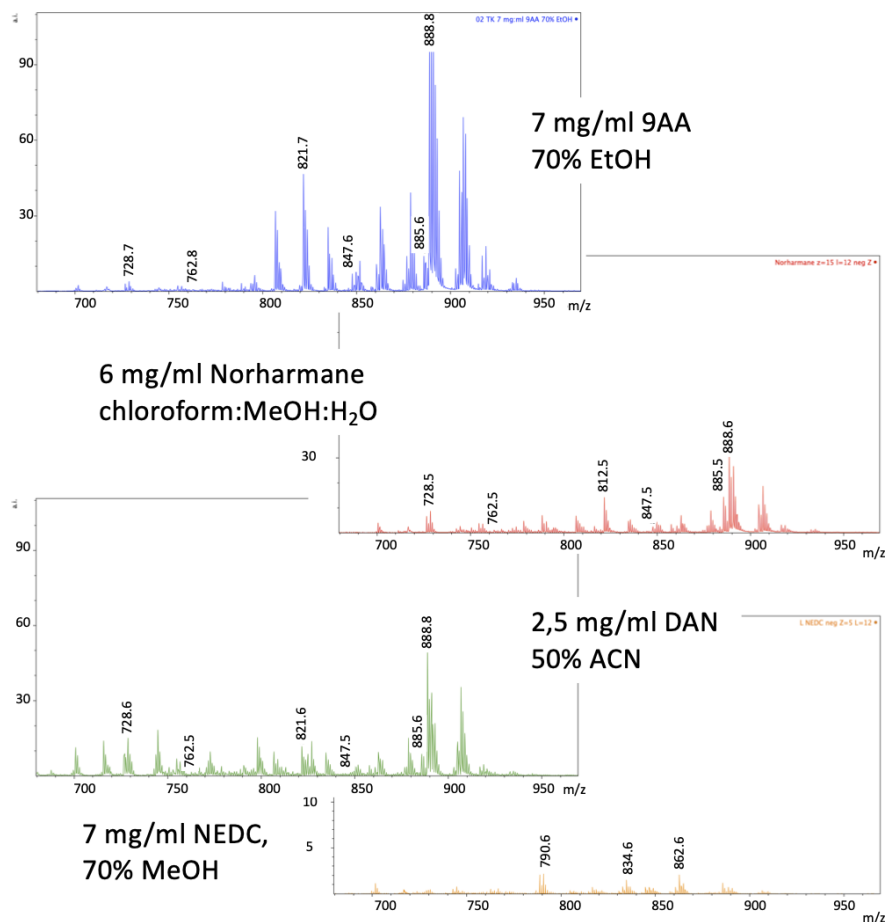


**Fig. 22** The mass spectra obtained with NEDC, norharmane, DAN and 9AA matrix.

Considering the performance of different matrices in the negative ionization mode (Fig. 22), norharmane matrix could be rejected since it has low peaks intensity and, as a result, it loses the information from the low MW range (e.g., peaks from fatty acids). NEDC is even worse for low MW peaks, but at least it can provide the ion maps for specific substances like glucose, n-acetyl-aspartic acid, glucose-6-phosphate, glucose-3-phosphate, and glutamic acid. DAN matrix produces higher peaks intensity in a lower mass range and seems to provide more information than 9AA. Additionally, it provides quite high intensities and signal-to-noise ratios. So, we recommended NEDC for particular tasks such as glucose analysis, and DAN for the lipids analysis in negative ionization mode.

**Table 1.** Summary of sample preparation optimization with the aid of wet-interface matrix deposition device (SunCollect®) for MALDI MSI (L – the number of matrix layers, Z - different spraying nozzle height).

Matrix	Matrix concentration	Solvent	Z	L
DHB	25 mg/ml	50% MeOH, 0.2% TFA	5	12
Norharmane	6 mg/ml	Chloroform:MeOH:H <sub>2</sub> O (1:1:1)	1; 25	14
DAN	2.5 mg/ml	50% ACN	5	14

Matrix	Matrix concentration	Solvent	Z	L
9AA	7 mg/ml	70% EtOH	5	14
NEDC	7 mg/ml	70% MeOH	5	12
Norharmane	6 mg/ml	Chloroform:MeOH:H2O (1:1:1)	15	12
DAN	2.5 mg/ml	50% ACN	1	16

## Conclusions

Wet-interface matrix deposition devices for MALDI mass spectrometry imaging are convenient and highly effective in use. Proper optimization of parameters such as the number of matrix layers and the nozzle height over the sample allows substantial improvement of the analysis parameters. Thus, the analysis of precious biological samples can be performed with the best possible quality. However, the care must be taken during the matrix selection to visualize the molecules of interest without losing their spatial distribution. Moreover, our analysis shows that the ion map obtained with the aid of a particular matrix might differ significantly with the use of another. So, care must be taken when comparing the results and drawing biological conclusions from such analyses.

**Funding:** This work was supported by the Polish National Science Center (NCN) grant number 2018/29/B/NZ4/02243 to ABK, statutory funds from the Maj Institute of Pharmacology at the Polish Academy of Sciences to PM, subsidy no 16.16.160.557 of the Polish Ministry of Science and Education to ABK, PS, PK and IK.

**Institutional Review Board Statement:** The study was conducted according to the guidelines of the Declaration of Helsinki and approved by the Local Ethics Committee (agreement number 137/2018).

**Data Availability Statement:** All the data present in the study are available upon request from the corresponding author.

**Conflicts of Interest:** The authors declare no conflict of interest. The funders had no role in the design of the study; in the collection, analyses, or interpretation of data; in the writing of the manuscript, or in the decision to publish the results.

## References

- 1 M. Dufresne, N. H. Patterson, J. L. Norris and R. M. Caprioli, *Anal Chem*, 2019, **91**, 12928–12934.
- 2 S. R. Shanta, C. S. Choi, J. H. Lee, C. Y. Shin, Y. J. Kim, K.-H. Kim and K. P. Kim, *J Lipid Res*, 2012, **53**, 1823–1831.
- 3 M. Visscher, A. M. Moerman, P. C. Burgers, H. M. M. Van Beusekom, T. M. Luider, H. J. M. Verhagen, A. F. W. Van der Steen, K. Van der Heiden and G. Van Soest, *J Am Soc Mass Spectrom*, 2019, **30**, 1790–1800.
- 4 M. K. Andersen, T. S. Høiem, B. S. R. Claes, B. Balluff, M. Martin-Lorenzo, E. Richardsen, S. Krossa, H. Bertilsson, R. M. A. Heeren, M. B. Rye, G. F. Giskeødegård, T. F. Bathen and M.-B. Tessem, *Cancer Metab*, 2021, **9**, 9.
- 5 Y. Chen, Y. Liu, J. Allegood, E. Wang, B. Cachón-González, T. M. Cox, A. H. Merrill and M. C. Sullards, *Methods Mol Biol*, 2010, **656**, 131–146.
- 6 P. Mielczarek, T. Slowik, J. H. Kotlinska, P. Suder and A. Bodzon-Kulakowska, *Molecules*, 2021, **26**, 2737.
- 7 H.-Y. J. Wang, C. B. Liu, H.-W. Wu and J. S. Kuo, *Rapid Commun Mass Spectrom*, 2010, **24**, 2057–2064.
- 8 A. J. Scott, B. Flinders, J. Cappell, T. Liang, R. S. Pelc, B. Tran, D. P. A. Kilgour, R. M. A. Heeren, D. R. Goodlett and R. K. Ernst, *Pathog Dis*, 2016, **74**, ftw097.

- 9 M. Dilillo, R. Ait-Belkacem, C. Esteve, D. Pellegrini, S. Nicolardi, M. Costa, E. Vannini, E. L. de Graaf, M. Caleo and L. A. McDonnell, *Sci Rep*, 2017, **7** , 603.
- 10 B. Rocha, B. Cillero-Pastor, G. Eijkel, V. Calamia, P. Fernandez-Puente, M. R. L. Paine, C. Ruiz-Romero, R. M. A. Heeren and F. J. Blanco, *Mol Cell Proteomics*, 2020, **19** , 574–588.
- 11 S. A. Noh, S.-M. Kim, S. H. Park, D.-J. Kim, J. W. Lee, Y. G. Kim, J.-Y. Moon, S.-J. Lim, S.-H. Lee and K. P. Kim, *J Proteome Res*, 2019,**18** , 2803–2812.
- 12 M. R. Eveque-Mourroux, P. J. Emans, R. R. M. Zautsen, A. Boonen, R. M. A. Heeren and B. Cillero-Pastor, *Analyst*, 2019, **144** , 5953–5958.
- 13 F. P. Y. Barré, B. S. R. Claes, F. Dewez, C. Peutz-Kootstra, H. F. Munch-Petersen, K. Grønbaek, A. H. Lund, R. M. A. Heeren, C. Côme and B. Cillero-Pastor, *Anal Chem*, 2018, **90** , 14198–14206.
- 14 A. R. Korte and Y. J. Lee, *J Mass Spectrom*, 2014, **49** , 737–741.
- 15 H. Liu, R. Chen, J. Wang, S. Chen, C. Xiong, J. Wang, J. Hou, Q. He, N. Zhang, Z. Nie and L. Mao, *Anal Chem*, 2014, **86** , 10114–10121.
- 16 M. Girod, Y. Shi, J.-X. Cheng and R. G. Cooks, *J Am Soc Mass Spectrom*, 2010, **21** , 1177–1189.
- 17 X. Lou, J. L. J. van Dongen and E. W. Meijer, *J Am Soc Mass Spectrom*, 2010, **21** , 1223–1226.
- 18 A. Bodzon-Kulakowska, A. Antolak, A. Drabik, M. Marszalek-Grabska, J. Kotlińska and P. Suder, *Biochim Biophys Acta Mol Cell Biol Lipids*, 2017,**1862** , 686–691.
- 19 P. M. Angel, J. M. Spraggins, H. S. Baldwin and R. Caprioli, *Anal Chem*, 2012, **84** , 1557–1564.
- 20 M. Strohal, D. Kavan, P. Novák, M. Volný and V. Havlíček, *Anal Chem*, 2010, **82** , 4648–4651.
- 21 H. Yang, W. Ji, M. Guan, S. Li, Y. Zhang, Z. Zhao and L. Mao, *Metabolomics*, 2018, **14** , 50.

